Birch pollen profilin: structural organization and interaction with poly-(L-proline) peptides as revealed by NMR

Tobias Domke[a], Torsten Federau[a], Kathrin Schlüter[b], Klaudia Giehl[1,b], Rudolf Valenta[c], Dietmar Schomburg[2,a], Brigitte M. Jockusch[b,*]

[a] *Molecular Structure Research, Gesellschaft für Biotechnologische Forschung, Mascheroder Weg 1, D-38124 Braunschweig, Germany*
[b] *Cell Biology, Zoological Institute, Technische Universität Braunschweig, D-38092 Braunschweig, Germany*
[c] *Institute of General and Experimental Pathology, University of Vienna, Währinger Gürtel 18-20, A-1090 Vienna, Austria*

Received 5 May 1997; revised version received 4 June 1997

Abstract The secondary structure of birch pollen profilin, a potent human allergen, was elucidated by multidimensional nuclear magnetic resonance (NMR), as a prerequisite to study the interaction of this profilin with ligands for its poly-(L-proline) (PLP)-binding site. The chemical shifts of the ^{15}N-labeled backbone amide groups were used to monitor complex formation with various PLP peptides. Titration with deca-L-proline (P_{10}) yielded a K_D of 0.2 mM. P_8 was the shortest PLP to provoke a significant reaction. $(GP_5)_3G$ bound significantly, confirming the interaction between profilins and the protein VASP containing this motif. Birch profilin interacted also with GP_6GP_5, found in the cyclase-associated protein (CAP), a suspected profilin ligand.

Key words: Birch profilin; Nuclear magnetic resonance; Poly-(L-proline) motif; Microfilament; Signal transduction

1. Introduction

Profilins [1] are proteins involved in microfilament dynamics. They bind to actin of various species, to phosphatidylinositol-4,5-bisphosphate (PIP_2) and to poly-(L-proline) (PLP; cf. [2] for original references). For example, birch pollen profilin binds to plant and animal actins [3,4], PIP_2 [5] and PLP [6]. The binding sites of actin and the signaling molecule PIP_2 on profilins overlap, precluding simultaneous binding of these ligands (cf. [2,7,8]). Hence, shuttling between actin and PIP_2 binding may enable profilins to act as a molecular switch between signal transduction and the membrane-apposed microfilament system [2,7,8]. In contrast, the PLP-binding site, located at the opposite face of the molecule can operate independently of the actin- and PIP_2-binding domains (cf. [9]). The vasodilator-stimulated phosphoprotein (VASP), a proline cluster-rich [10], microfilament-associated [11] protein, was identified as the first biologically relevant ligand for this profilin domain [10]. Since VASP is a substrate of cAMP/cGMP-dependent protein kinases [12], complexes between profilin and VASP or VASP-like proteins [13] may link profilin to the adenylyl cyclase signaling route. Additionally, several PLP-rich formin-related proteins were identified as profilin ligands [14–16], some of which also interact with Rho-related small GTPases [14,16,17]. Hence, regulation of the microfilament system by different signaling pathways may involve physical contact between profilins and various PLP-containing proteins in yeast and animal cells. For plant cells, this is much less clear. The 3-dimensional (3D) structure of two plant profilins has been recently elucidated (*Arabidopsis* and birch profilin, cf. [18,19]), but detailed information on their interactions with signaling proteins via the PLP-binding domain is still missing.

In this study, we provide data which contribute to answering this question. We first established the secondary structure of birch pollen profilin by NMR and found it remarkably similar to the NMR structure of *Acanthamoeba* profilin I [20]. Subsequently, we used the chemical shifts of the ^{15}N-labeled backbone amide groups to characterize the profilin binding of PLP peptides and derivatives occurring in various proteins.

2. Materials and methods

2.1. Sample preparation

Birch profilin was expressed in *Escherichia coli* BL21(DE3), using a T7-RNA-polymerase system and birch profilin cDNA subcloned in the pMW175 expression vector [4]. Bacteria were grown in M9-minimal medium supplemented with minerals. Proteins were labelled with either ^{15}N or with both ^{15}N and ^{13}C by providing $^{15}NH_4Cl$ (1 g/l) as the sole nitrogen source and [$^{13}C_6$]-D-glucose (2 g/l) as the sole carbon source. Profilin expression was induced with 1 mM isopropyl thiogalacto-pyranosid (IPTG) and allowed to continue for 4–5 h at 37°C and 220 rpm. The protein was purified from bacterial extracts by PLP affinity chromatography essentially as described [4]. Approximately 13 mg of purified ^{15}N or ^{15}N/^{13}C-enriched birch profilin was obtained from 1 l of bacterial culture. Prior to NMR spectroscopy, 50 μl of D_2O was added and the solution adjusted to 0.8 mM profilin.

PLP-peptides were synthesized with acetylated N-termini and amidated C-termini on an Applied Biosystems peptide synthesizer (Perkin-Elmer, Foster City, CA) by a stepwise solid-phase procedure, using FMOC chemistry. They were incubated with profilin in a 2-fold molar excess (0.2 mM peptide to 0.1 mM profilin). For titration with P_{10}, spectra were taken with samples containing 0.05, 0.1, 0.2, 0.3, 0.5, and 0.75 mM P_{10} and 0.1 mM profilin.

2.2. NMR spectroscopy

Birch profilin was found to be of limited solubility and prone to irreversible aggregation at concentrations higher than 0.8 mM and elevated temperatures. Therefore, the samples were not further concentrated and spectra were acquired at 293 K only. Under these conditions, samples were stable for approximately 7 days. Freshly saturated solutions of the uniformly ^{15}N/^{13}C-labelled protein were prepared in H_2O/D_2O (9:1) at pH 6.5. All multidimensional NMR spectra were recorded without spinning on a Bruker AVANCE DMX 600 NMR spectrometer equipped with a 10 G/cm gradient unit. Data were processed with UXNMR and AURELIA (Bruker Rheinstetten,

*Corresponding author.

[1] *Present address:* Universität Ulm, Klinikum, Robert-Koch-Str. 8, D-89081 Ulm, Germany.

[2] *Present address:* Universität zu Köln, Biochemie, Zülpicher Str. 47, D-50674 Köln, Germany.

PII S0014-5793(97)00719-9

Germany) on a Silicon Graphics workstation. Peak lists were evaluated and compared with the program EXCEL (MicroSoft, USA).

A standard backbone assignment strategy [21] was followed, using CT-HNCO, CT-HNCA, CT-HN(CO)CA, CT-HN(CA)CO, CT-HN(CO)CAHA, CT-HN(CA)HA, ^{15}N-edited NOESY and TOCSY spectra. The spectral width for CO was 19.9 ppm, for CA 25.3 ppm, for HA 3.4 ppm, for HN 6.4 ppm and for ^{15}N 31.0 ppm. The carrier was set to 56.0 ppm (^{13}Cα), 50.0 ppm (^{13}Cα,β), 175.5 ppm (^{13}CO), 116.6 ppm (^{15}N) and 4.81 ppm (^{1}H), and 8.9 ppm ($^{1}H^{N}$) in all triple resonance experiments and 4.75 ppm (^{1}H) for ^{15}N-edited NOESY and TOCSY spectra. No HCA type spectrum was taken, as the samples could not be lyophilised to obtain a D_2O sample. A 3-9-19 water-suppression pulse sequence [22] was used in all experiments, except for the 2D and 3D NOESY and TOCSY experiments where presaturation was employed.

The ^{1}H chemical shifts were referenced to a hypothetical internal sodium 3-(trimethylsilyl)-propionate (TSP) standard and the heteronuclear chemical shifts were calculated from this, using the ratio $\gamma^{13}C/\gamma^{1}H$ and $\gamma^{15}N/\gamma^{1}H$ [23]. The differences of the ^{13}CO, ^{13}Cα and ^{1}Hα chemical shifts from standard values for random coil conformation were calculated using standard procedures.

The chemical shifts of the backbone amide protons were taken from the 2D ^{15}N HSQC spectrum and ^{13}Cα shifts from the CT-HNCA and CT-HN(CO)CA spectra. The ^{13}CO chemical shifts of the backbone were obtained from the HN(CA)CO spectrum. This was supplemented with information for the ^{13}CO of the proceeding residue from the HNCO spectrum. It was necessary to assign the ^{1}Hα chemical shifts from a combination of several spectra (CT-HN(CA)HA, the CT-HN(COCA)HA and the ^{15}N edited TOCSY-HMQC spectra), as the poor responses in the TOCSY spectra precluded direct assignments. Hence, amino acid spin systems were identified by using the partial correlations of the 2D TOCSY, the ^{15}N-edited TOCSY-HMQC spectra and the ^{13}Cβ chemical shifts from the CT-HNCACB. Initially, these data resulted in sequential assignments of subclusters of up to seven residues. In the final analysis, these were combined to furnish the full backbone assignment, apart from M1, E48 and G90 which could not be unambiguously assigned. The assignments were substantiated by the CT-HNCA spectrum.

To establish the secondary structure of birch profilin, the difference between the chemical shifts of ^{13}CO, ^{13}Cα and ^{1}Hα and the random coil values was used [24,25]. A combination of the shift differences was performed by initially normalizing the shift differences $\Delta\delta(^{13}CO)$, $\Delta\delta(^{13}C\alpha)$ and $\Delta\delta(^{1}H\alpha)$ by dividing each value by the average differences for the corresponding nuclei species. Then the normalized values of $\Delta\delta(^{13}CO)$ and $\Delta\delta(^{13}C\alpha)$ were added and $\Delta\delta(^{1}H\alpha)$ was subtracted to give the combined shift difference Δδ(all). No smoothing was applied in order to avoid ambiguities in regions possessing short secondary structural elements. These data, supported by the medium-range NOE data, were used to determine position and extension of secondary structural elements.

3. Results

3.1. The secondary structure of birch profilin is closely related to that of Acanthamoeba profilin I

The normalized values for the individual chemical shift differences, $\Delta\delta(^{1}H\alpha)$, $\Delta\delta(^{13}C\alpha)$ and $\Delta\delta(^{13}CO)$ are shown in Fig. 1. Slight ambiguities in the single shift differences Δδ of ^{1}Hα, ^{13}Cα and ^{13}CO could be resolved by combining the shift differences to Δδ(all) [26], as is also depicted in Fig. 1.

In a final step, the information derived from the chemical shift differences was combined with the NOE data from the ^{15}N edited NOESY spectra to unambiguously define the secondary structural elements. Hence, strong $NN_{(i,i+1)}$ NOE signals, the presence of $\alpha N_{(i,i+3)}$ NOE signals and positive $\Delta\delta(all) > +0.3$ of at least four consecutive residues were interpreted as an α-helix. Strong $\alpha N_{(i,i+1)}$ NOE signals, the absence of $NN_{(i,i+1)}$ NOE signals and $\Delta\delta(all) < +0.3$ for at least three consecutive residues were interpreted as a β-strand. The resulting secondary structure is summarized in Fig. 2. In conclusion, the experimental NMR data for birch profilin provide

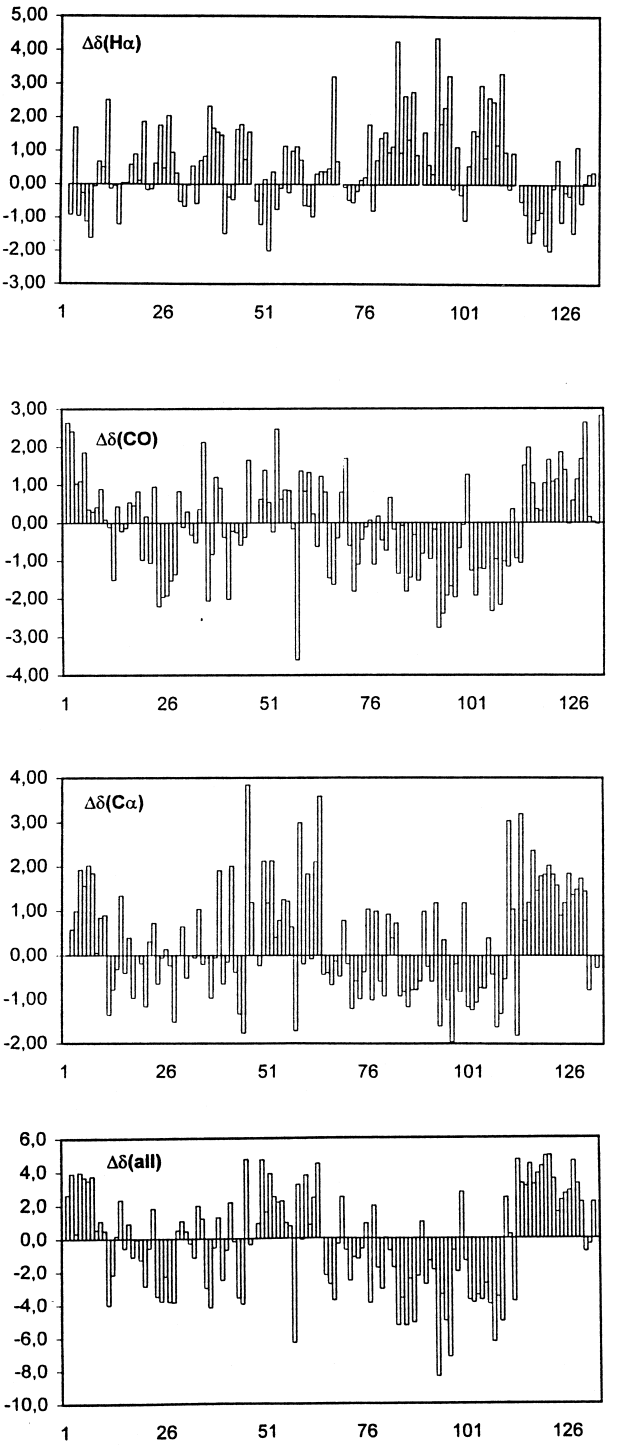

Fig. 1. Plots of the normalized chemical shift differences, $\Delta\delta(^{1}H)$, $\Delta\delta(^{13}C\alpha)$ and $\Delta\delta(^{13}CO)$, and the combined shift differences Δδ(all). Regions with negative peaks for $\Delta\delta(^{1}H)$ and with positive peaks for $\Delta\delta(^{13}C)$ and $\Delta\delta(^{13}CO)$ are interpreted as helical or extended regions. Regions with the reversed sign combination are indicators of β-strands.

direct evidence of the positions and length of three α-helices and seven β-strands, which is in agreement with the X-ray analysis of birch profilin crystals [19]. Minor differences comprise the exact length of α-helices and β-strands as determined with both methods. Analogous small discrepancies have been

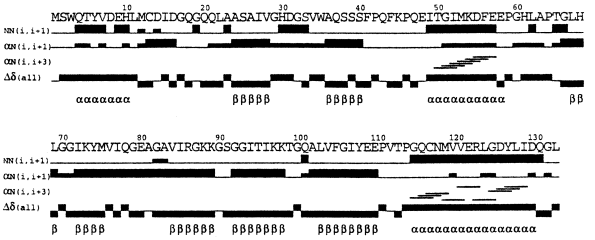

Fig. 2. Composite plot of the Δδ_(all) sign, the short range NOEs $NN_{(i,i+1)}$ and $\alpha N_{(i,i+1)}$ and $\alpha N_{(i,i+3)}$ used for deducing the secondary structure elements. The NOEs were taken from the 3D ^{15}N edited NOESY spectrum and the horizontal line widths represent their magnitudes which have been classified as strong, medium and weak.

observed before for NMR and X-ray data of *Acanthamoeba* profilin I (cf. [20] with [27]).

The secondary structure elements thus identified in birch profilin (Fig. 2) are quite similar to human profilin I [28] and strikingly similar to those determined by NMR for *Acanthamoeba* profilin I [20]. In fact, small differences may even be due to differences in the experimental setup, such as using different temperatures. The α-helix 1 (Q4 to H10) of birch profilin is two residues longer than that of *Acanthamoeba* profilin I, and five additional residues are inserted between α-helix 1 and β-strand 1 of birch profilin. No $\alpha N_{(i,i+3)}$ NOE signals were found in this region, but it is defined by large Δδ(all) values and $NN_{(i,i+1)}$ NOE signals. β-Strand 1 (A24 to V28) is very similar in length and position in birch and *Acanthamoeba* profilin I, while β-strand 2 (A36 to S40) is one residue longer in the *Acanthamoeba* protein. Although the Δδ(all) value of S39 is positive, the $\alpha N_{(i,i+1)}$ NOE signals show that the end of β-strand 2 is at S40. α-helix 2 (I49 to E58), defined by strong $NN_{(i,i+1)}$, $\alpha N_{(i,i+2)}$ and $\alpha N_{(i,i+3)}$ NOE signals, matches the same element in *Acanthamoeba* profilin I, but is shorter by one residue. The $NN_{(i,i+1)}$ NOE signals and the Δδ(all) suggest a short helix-like turn between L62 and P64. This is the counterpart of a helical region found in *Acanthamoeba* profilin I at this position [20]. The position of β-strands 3 (L67 to L69) and 4 (I72 to M75) are equivalent to β-strands 3 and 4 of *Acanthamoeba* profilin I [20]. The beginning of β-strand 5 (V84 to K89) is delineated by the absence of $NN_{(i,i+1)}$ and the presence of $\alpha N_{(i,i+1)}$ NOE signals. The position of β-strand 6 (G92 to K98) is given by $\alpha N_{(i,i+1)}$ and negative Δδ(all) values. β-strand 7 (L103 to E110) is defined by the absence of $NN_{(i,i+1)}$ NOE signals at its beginning, and by the loss of the $\alpha N_{(i,i+1)}$ NOE signals and negative Δδ(all) values at its end. The C-terminal α-helix 3 (G115 to D130), again defined by $NN_{(i,i+1)}$ and $\alpha N_{(i,i+3)}$ NOE signals and positive Δδ(all) values, is three residues longer than in *Acanthamoeba* profilin I [20].

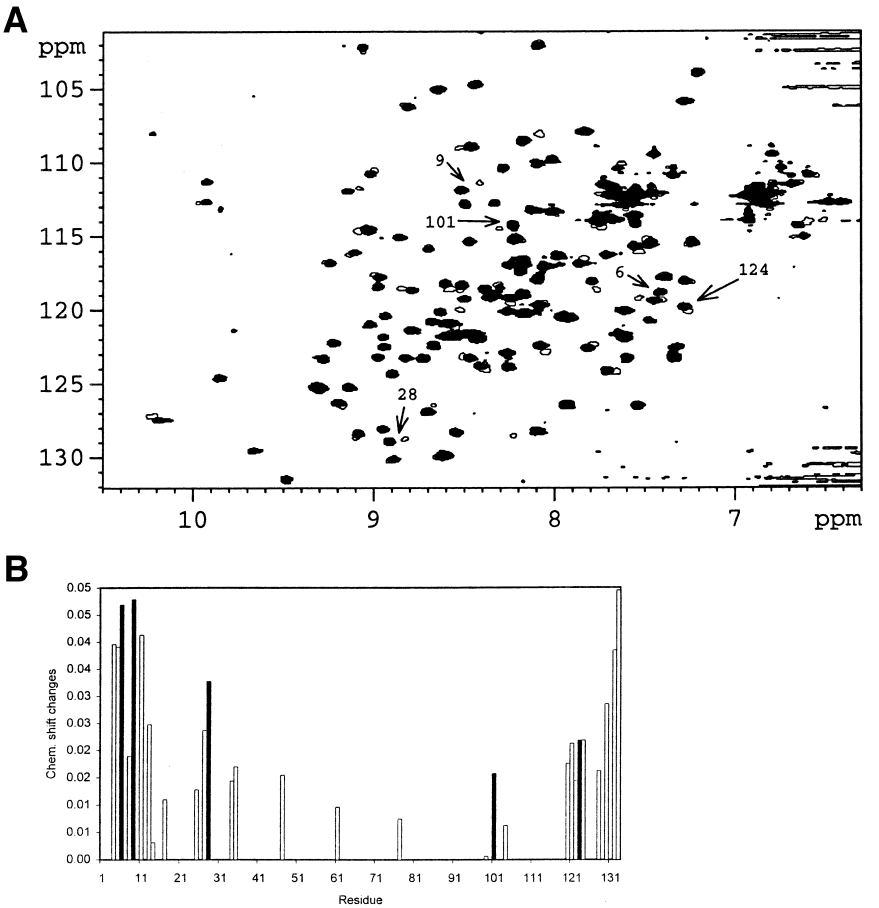

Fig. 3. Chemical shift changes of the backbone amide groups upon PLP binding. A: Detail of the ^{1}H-^{15}N HSQC spectra of birch profilin before and after the addition of P_{10}. Signals obtained upon the addition of P_{10} are marked in white. Numbers and arrows indicate individual amino acid residues considered further in (B) and in Fig. 4. B: Summarized normalized chemical shift changes of the backbone amide groups. The changes were calculated from HN-correlations of pure birch profilin and a spectrum of birch profilin incubated with P_{10} (molar ratio profilin/P_{10} was 1:2). The residues with strong signal shifts, indicated in black, were used for the analysis of binding to PLP peptides (cf. Fig. 4).

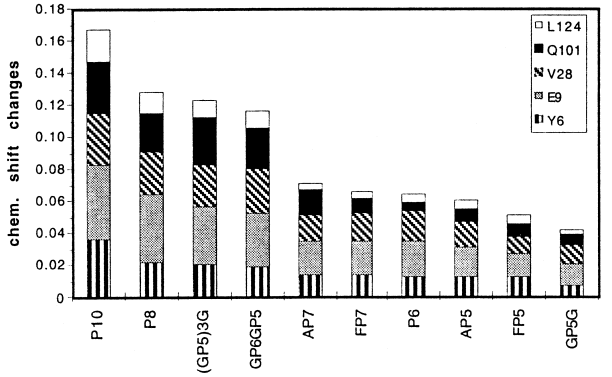

Fig. 4. Plot of the summed normalized chemical shift changes of the backbone amide groups, as observed for birch profilin residues Y6, E9, V28, Q101, L124 upon the addition of the peptides indicated underneath each bar.

3.2. *The affinity of birch profilin for PLP is similar to other profilins*

The affinity of birch profilin for PLP was analysed by incubating the protein (0.1 mM) with 0.2 mM of the proline decamer, P_{10}. The ^{15}N and ^{1}H chemical shift differences of the amide groups were determined. These differences were normalized and summed, using the function $0.5[(\Delta_{NH})^2+(\Delta_N/5)^2]^{1/2}$ [26]. Analogous to previous results obtained for *Acanthamoeba* profilin I [29], numerous amino acid residues displayed changes upon binding of the P_{10} peptide to birch profilin, as seen in the ^{1}H-^{15}N-HSQC spectra (Fig. 3A). These reactive residues were clustered in the N- and C-terminal region (Fig. 3B) and were also located within the PLP-binding area determined for human [9] and *Acanthamoeba* profilin I [29]. Titration of birch profilin with various concentrations of P_{10} and Scatchard analysis of the chemical shift changes of N_ε, H_ε and $H_{\varepsilon 2}$ of Q116 yielded values of 0.14, 0.17 and 0.15 mM, respectively. Hence, the K_D value of this interaction is approximately 0.2 mM, which is again quite similar to the K_D value of 0.4 mM of *Acanthamoeba* profilin I–P_{10} complexes [29].

3.3. *The PLP–profilin interaction is primarily determined by the length of the PLP peptide*

We determined the length of the PLP stretch needed to provoke a significant change in chemical shifts. The backbone amide shift changes of five residues, Y6, E9, V28, Q101, L124 (indicated in black in Fig. 3B) were used to compare the changes induced by polyproline peptides of varying length and composition. When peptides consisting of 8 or 6 proline residues (P_8 and P_6, respectively) were offered instead of P_{10}, the chemical shift changes were reduced, as seen in Fig. 4. P_8 induced still two-thirds of the overall changes in these five amino acid residues as compared to P_{10}. The main difference between the changes provoked by P_{10} and P_8 were confined to Y6. For this single residue, the replacement of P_{10} by P_8 decreased the changes to approximately 50% (Fig. 4). With P_6, the overall signal changes in all five residues considered were decreased to roughly half of the value obtained with P_{10} (Fig. 4). Thus, at least eight continuous proline residues were needed to provoke a substantial reaction.

We then measured the chemical shifts induced by peptides designed after various microfilament proteins which are either already identified or suspected profilin ligands: GP_5 and $(GP_5)_3G$, both contained in VASP [11], GP_6GP_5, which is found in the cyclase-associated protein CAP [30,31], AP_7, a constituent of ezrin [32], FP_5, a motif present in vinculin [33], and AP_5, a sequence present in the insect troponin H34 [34]. As seen in Fig. 4, the $(GP_5)_3G$ VASP motif and the GP_6GP_5 CAP sequence provoked signal shifts in the same range as P_8. On the other hand, the single GP_5G of VASP, AP_7, AP_5 and FP_5 all showed a much weaker reaction with the relevant birch profilin residues, comparable to the reaction obtained with P_6. For the peptides P_{10}, $(GP_5)_3G$ and AP_7, the measurements were repeated, using freshly labeled and purified protein. The results were almost identical. Hence, the effects seen were reliable, revealing that the heteropeptides used could be assigned to two classes: they either provoked a P_{10}/P_8-like reaction, or a low, P6-like reaction. Within each class, the reaction did not substantially differ with the peptide. An additional flanking residue, like F or A at the N-terminal end of FP_7 or AP_7, respectively, did not lead to marked alterations in the chemical shift changes. From these data, we concluded that the main feature determining the reaction was the total length of the proline stretch, but interruptions by single glycine residues were tolerated.

4. Discussion

The structural features of various profilins have been analysed by multidimensional NMR spectroscopy [20,28] and X-ray crystallography ([18,19,27,35] and references therein). This NMR study contributes the secondary structural elements of birch profilin in solution, and our data agree well with the number and position of these elements as determined in the crystallized protein [19].

In a comparison of 35 profilin sequences, it was seen that of the 18 highly conserved residues, eight are involved in PLP binding [18]. Hence, the PLP-binding site seems the most conserved region among profilins, including birch profilin. On the other hand, the tertiary structure of birch profilin, as deduced from the crystal, shows a significant difference between birch and all other profilin structures elucidated so far: α-helix 1 in the crystallized birch protein was found arranged not in parallel with the C-terminal helix, but oriented perpendicular to it [19]. Since both helices participate in PLP binding, such an arrangement should cause the birch profilin to bind less well to PLP than other profilins. Our findings that the dissociation constant for birch pollen profilin and P_{10} is very similar to that found for *Acanthamoeba* profilin I, and that birch, bovine and human profilin bind equally well to human protein VASP [10] argue against this interpretation. These discrepancies might either point to an anomalitiy caused by crystallization, or to a flexible α-helix 1 in the birch protein which in solution might change its orientation to participate in PLP binding.

The dissociation constant 0.2 mM for birch profilin/P_{10}, as determined here, agrees well with the value determined for *Acanthamoeba* profilin I/PLP [29], and, again in analogy to *Acanthamoeba* [7], PLP stretches shorter than P_8 did not effectively bind. Our findings that Y6, one of the few conserved residues among profilins, reacts very strongly to changes in the peptide length emphasizes the importance of this residue for PLP binding.

By NMR analysis, we confirmed the binding of the VASP motif $(GP_5)_3G$ to birch profilin [10], while the single GP_5G motif is an inefficient ligand. In addition, we provide evidence

for a complex formation of the GP_6GP_5 motif of CAP [31] with profilin. CAP–profilin interaction has been suspected from genetic studies showing a functional link between CAP and profilin in yeast [36]. Recently, and independently of our studies, the interaction of the CAP peptide GP_6GP_5 with bovine profilin I has also been demonstrated by fluorescence spectroscopy [37]. While both these sets of data point to CAP as a profilin ligand, an interaction of intact CAP with either bovine or birch profilins was not seen in experiments using the two hybrid system or by affinity chromatography (our own unpublished results). We suspect, but cannot prove at the moment, that CAP contains a cryptic profilin-binding site analogous to cryptic ligand-binding sites described for vinculin or ezrin. These proteins occur normally in a folded, dormant configuration (for references, see [38]), and there is evidence that the same is true for CAP [39]. In contrast, neither AP_7 derived from ezrin nor the vinculin motif FP_5 showed a significant reaction with profilin, which is consistent with data demonstrating no binding of purified ezrin, troponin H34 or vinculin to profilins by affinity chromatography (our own unpublished results). Thus, our data show that NMR is a reliable technique to determine PLP–profilin interaction and may be used to identify further protein ligands for the PLP-binding site of profilins from yeast, animals and plants.

Acknowledgements: We are grateful to Drs. Mark Susani (Salzburg) for the birch profilin construct, Victor Wray and Roland Frank (GBF, Braunschweig) for peptide synthesis and to Christel Kakoschke for expert technical assistance. We thank Dr. S.C. Almo (A. Einstein College of Medicine, New York) for providing the X-ray data on crystallized birch pollen profilin prior to publication. This study was supported by the Deutsche Forschungsgemeinschaft (grant to B.M.J.) and the Austrian Science Foundation (grant to R.V.).

References

[1] L. Carlsson, L. Nystrom, I. Sundkvist, F. Markey, and U. Lindberg, in: S.V. Perry et al. (Ed.), Contractile Systems in Non-Muscle Tissues. North Holland Publ., Amsterdam, 647 (1976) 29.
[2] K. Schlüter, B.M. Jockusch, and M. Rothkegel, Biochim. Biophys. Acta, (1997) in press.
[3] Valenta, R. et al. (1993) J. Biol. Chem. 268, 22777–22781.
[4] Giehl, K., Valenta, R., Rothkegel, M., Ronsiek, M., Mannherz, H.G. and Jockusch, B.M. (1994) Eur. J. Biochem. 226, 681–689.
[5] Drobak, B.K. and Watkins, P.A. (1994) Biochem. Biophys. Res. Commun. 205, 739–745.
[6] Valenta, R. et al. (1991) Science 253, 557–560.
[7] Machesky, L.M. and Pollard, P.D. (1993) Trends Cell Biol. 3, 381–385.
[8] Sohn, R.H. and Goldschmidt-Clermont, P.J. (1994) BioEssays 16, 465–472.
[9] Metzler, W.J., Bell, A.J., Ernst, E., Lavoie, T.B. and Mueller, L. (1994) J. Biol. Chem. 269, 4620–4625.
[10] Reinhard, M., Giehl, K., Abel, K., Haffner, C., Jarchau, T., Hoppe, V., Jockusch, B.M. and Walter, U. (1995) EMBO J. 14, 1583–1589.
[11] Haffner, C., Jarchau, T., Reinhard, M., Hoppe, J., Lohmann, S.M. and Walter, U. (1995) EMBO J. 14, 19–27.
[12] Eigenthaler, M. and Walter, U. (1994) Thromb. Haemorrh. Disord. 8, 41–46.
[13] Gertler, F.B., Niebuhr, K., Reinhard, M., Wehland, J. and Soriano, P. (1996) Cell 87, 227–239.
[14] Evangelista, M., Blundell, K., Longtine, M.S., Chow, C.J., Adames, N., Pringle, J.R., Peter, M. and Boone, C. (1997) Science 276, 118–122.
[15] Chang, F., Drubin, D. and Nurse, P. (1997) J. Cell Biol. 137, 169–182.
[16] N. Watanabe et al. EMBO J. (1997) in press.
[17] Kohno, H. et al. (1996) EMBO J. 15, 6060–6068.
[18] Thorn, K.S., Christensen, H.E.M., Shigeta Jr., R., Huddler Jr., D., Shalaby, L., Lindberg, U., Chua, N.H. and Schutt, C.E. (1997) Structure 5, 19–32.
[19] Fedorov, A.A., Ball, T., Mahoney, N.M., Valenta, R. and Almo, S.C. (1997) Structure 5, 33–45.
[20] Vinson, V.K., Archer, S.J., Lattman, E.E., Pollard, T.D. and Torchia, D.A. (1993) J Cell Biol 122, 1277–1283.
[21] G.M. Clore, and A.M. Gronenborn, CRC Press, Boca Raton, FL, 1993.
[22] Sklenar, V., Piotto, R., Lepik, S. and Saudek, V. (1993) J. Magn. Res. Series A 102, 241–245.
[23] Ikura, M., Kay, L.E., Sparks, S.W., Torchia, D.A. and Bax, A. (1989) Biochemistry 30, 5498–5504.
[24] Spera, S. and Bax, A. (1991) J. Am. Chem. Soc. 113, 5490–5492.
[25] Wishart, D.S. and Sykes, B. (1994) Methods Enzymol. 239, 363–392.
[26] Grzesiek, S., Bax, A., Clore, G.M., Gronenborn, A., Hu, J.S., Kaufman, J., Stahl, S.J. and Wingfield, P.T. (1996) Nature Struct. Biol. 3, 340–345.
[27] Fedorov, A.A., Magnus, K.A., Graupe, M.H., Lattman, E.E., Pollard, T.D. and Almo, S.C. (1994) Proc. Natl. Acad. Sci. USA 91, 8636–8640.
[28] Metzler, W.J., Constantine, K.L., Friedrichs, M.S., Bell, A.J., Ernst, E.G., Lavoie, T.B. and Mueller, L. (1993) Biochemistry 32, 13818–13829.
[29] Archer, S.J., Vinson, V.K., Pollard, T.D. and Torchia, D.A. (1994) FEBS Lett. 337, 145–151.
[30] Voijtek, A.B. and Cooper, J.A. (1993) J. Cell Sci. 105, 777–785.
[31] Matviw, H., Yu, G. and Young, D. (1992) Mol. Cell Biol. 12, 5033–5040.
[32] Gould, K.L., Bretscher, A., Esch, F.S. and Hunter, T. (1989) EMBO J. 8, 4133–4142.
[33] Coutu, M.D. and Craig, S.W. (1988) Proc. Natl. Acad. Sci. USA 85, 8535–8539.
[34] Karlik, C.C., Mahaffey, J.W., Coutou, M.D. and Fyrberg, E.A. (1984) Cell 37, 469–481.
[35] Schutt, C.E., Myslik, J.C., Rozycki, M.D., Goonesekere, N.C. and Lindberg, U. (1993) Nature 365, 810–816.
[36] Vojtek, A., Haarer, B., Field, J., Gerst, J., Pollard, T.D., Brown, S. and Wigler, M. (1991) Cell 66, 497–505.
[37] Lambrechts, A., Verschelde, J.L., Jonckheere, V., Goethals, M., Vandekerckhove, J. and Ampe, C. (1997) EMBO J. 16, 484–494.
[38] Jockusch, B.M. and Rüdiger, M. (1996) Trends Cell Biol. 6, 311–315.
[39] Hubberstey, A., Yu, G., Loewith, R., Lakusta, C. and Young, D. (1996) J. Cell Biochem. 61, 459–466.